OPTIMIZATION OF GEOMETRIC PARAMETERS OF THE VIBRO-PLANETARY MECHANISM

Umida Ziyamukhamedova[1], Sherali Mamayev[1], Jasurbek Nafasov[1], Shaozimova Umida[2], Turgunaliyev Elbek[1], Abdurakhimov Shokhjakhon[1]

[1]Tashkent State Transport University, Tashkent, Uzbekistan

[2]Tashkent State Technical University, Tashkent, Uzbekistan

Abstract

The subject of the research is the optimization of the vibro-planetary mechanism. In the article, based on the closure condition of the contours, equations for the projection of links onto the corresponding coordinate axes are formulated. A functional relationship has been established between the kinematic parameters characterizing the movement of the input and output links of the mechanism. The obtained numerical calculations are presented in the form of graphical dependencies. The aim of the work is to optimize the geometric parameters of the vibro-planetary mechanism. The conclusions obtained in the article can be used to improve and design modern technological equipment with mechanisms similar to the vibro-planetary mechanism.

Keywords: *vibro-planetary mechanism, kinematic diagram, analytical study of the mechanism, mathematical model, contour closure condition, metric synthesis of the mechanism, kinematic analysis of the mechanism, optimization, crank, rocker, rocker stone*

INTRODUCTION

In modern machine building, the role of mechanisms used in obtaining advanced materials is invaluable for the development of materials science. By improving material production technologies, it is possible to ensure the operational reliability of parts. Particularly, research in this field has shown that activating fillers of polymer-based composite materials before incorporating them into the composition improves the structural organization of the composite [1-4]. However, it should be emphasized that by enhancing existing methods [5-7] for activating fillers, it is possible to obtain mechanically stronger materials from existing materials. It has been determined that the proposed vibroplanetary activator for filler activation enhances the surface activity of particles more effectively than other methods, due to its simultaneous rotational and reciprocating motion during the activation process [8-11].

Mechanical activation of filler particles plays a crucial role in the formation of structures in composite materials, the enhancement of physical, mechanical, and operational properties of the material, and the creation of strong bonds between structures. The composition of natural minerals consists primarily of oxides with ionic bonds. During mechanical activation, the forces acting on the particles and their motion trajectories are key factors in determining the material's properties, influencing the formation of positively and negatively charged particles.

RESEARCH OBJECTS AND METHODS

A mechanochemical phenomenon comprises two main components: a mechanochemical process that determines the conversion of mechanical energy into chemical substances, and a mechanochemical process that releases mechanical energy due to chemical reactions. Today, the negative and positive charges formed during the mechanical activation of dispersed fillers in polymer composite materials participate in the physical and chemical processes occurring between layers during structure formation and influence the operational parameters of the material. Simultaneous activation of mechanically activated filler particles by two different forces acting in various directions leads to an improvement in the quality of the filler.

In the vibro-planetary mechanism (Figure 1), the reciprocating motion is provided by the guiding lever (6) fixed to the support and the stone (4), while the rotational motion is provided by the rotating lever (3) fixed to the electric motor shaft. The mechanoactivator (5) is attached to the stone as a detachable unit. The grinding balls (2) placed inside the mechanoactivator occupy 0.8 of its volume.

Our vibro-planetary grinder, constructed as a stand, is equipped with an electric motor (1) that can vary rotational speed from 750 rpm to 3000 rpm. This allows for obtaining results at different rotation frequencies and selecting the optimal frequency.

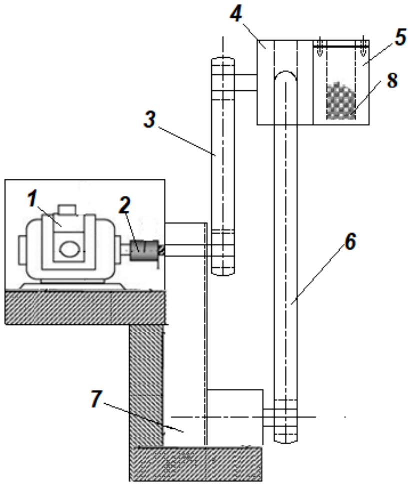

Fig. 1. General view of the vibro-planetary activator: 1 - electric motor; 2 - coupling; 3 - crankshaft; 4 - rock; 5 - mechanoactivator; 6 - guiding lever; 7 - grinder housing; 8 - grinding balls.

The operating principle of the vibro-planetary mechanism is based on the movement of a rocker mechanism, where an activation hopper - a mechanoactivator - is installed on the rocker stone. The activity of the particles increases as a result of the impact force of the filler-activating spheres on the filler particles inside the mechanoactivator. Consequently, the greater the impact force of the balls inside the mechanoactivator on the particles, the shorter the activation time and the higher the degree of particle activity.

The impact force of the balls inside the mechanoactivator depends on the Coriolis force generated in the mechanism's rocker stone, which increases in direct proportion to the increase in this force. To find the optimal value of the Coriolis force generated in the rocker stone, it is necessary to optimize the length and angular velocity of the crank of the vibro-planetary mechanism.

When determining the optimal value of the link lengths and the distance between the supports of the crank-slider mechanism, which is the main working component of the vibroplanetary activator, it is primarily necessary to determine the rational range of angular acceleration values for the output link of the mechanism.

For the kinematic analysis of the crank-slider mechanism shown in Figure 2, it is placed in a Cartesian coordinate system. By plotting the coordinates of the kinematic pairs along the x-axis and y-axis, we obtain the following equations for point A of the kinematic pair formed by the projections of the stone and the slider.

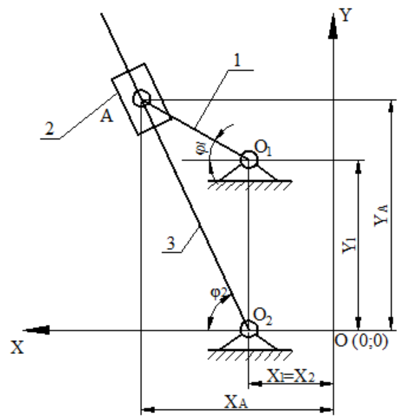

Fig. 2. Structural diagram of a vibro-planetary mechanism.

$$X_A = X_1 + O_1A\cos\varphi_1 = X_2 + O_2A\cos\varphi_2 \tag{1}$$

$$Y_A = Y_1 + O_1A\sin\varphi_1 = Y_2 + O_2A\sin\varphi_2 \tag{2}$$

Let's define the values given in the system of equations 1 and 2 above as follows:

$$O_1A = l_1;\ X_1 = X_2 + O_1O_2;\ y_1 = a;\ y_2 = 0;\ O_2A = B.$$

In that case, the system of equations 1 and 2 takes the following form:

$$X_A = X_1 + l_1\cos\varphi_1 = X_2 + B\cos\varphi_2 \tag{3}$$

$$Y_A = a + l_1A\sin\varphi_1 = B\sin\varphi_2 \tag{4}$$

Using the system of equations, we derive the following equation for the rotation angle φ_2 of the slider:

$$\cos\varphi_2 = b_1\ \cos\varphi_1 \tag{5}$$

$$\sin\varphi_2 = c_1\ + b_1\ \sin\varphi_1 \tag{5}$$

here, $b_1\ = \frac{l_1}{B};\ c_2\ = \frac{a}{B}$.

By squaring and adding the left and right sides of the system of equations 5 and 6, we obtain the following equality:

$$\sin\varphi_1 = \frac{1-c_2^2b_1^2}{2c_2b_1} \tag{7}$$

$$\varphi_1 = arcsin\varphi_1(\frac{1-c_2^2b_1^2}{2c_2b_1}) \tag{8}$$

φ_1 represents the change in the value of "B" at the turn and its dependence on the value of the distance "a" between the supports. Therefore, when determining the angular velocity ω_1 and angular acceleration ε_1 of the crankshaft, we must introduce the following change functions:

$X_1 = X_1(t);\ X_2 = X_2(t);\ Y_1 = Y_1(t);\ Y_2 = Y_2(t);$ ва $B = B(t)$.

By substituting the values of the above function into equation 8 and differentiating them with respect to time, we obtain the following:

$$\omega_1 = \frac{d\varphi_1}{dt} \qquad \text{ва} \qquad \varepsilon = \frac{d^2\,\varphi_1}{dt^2}$$

To solve these equations, it is necessary to designate the kinematic pairs O_1 and O_2 as fixed, in which case the distance between them:

$O_1O_2 = a = const$ is equal to. In that case, we substitute the values of all variable functions into equation 8:

$$\varphi_1 = \arcsin\left[\frac{1-\frac{a^2}{B^2}-\frac{l_1^2}{B^2}}{\frac{2al_1}{B^2}}\right] = \arcsin\left[\frac{B^2-(a^2+l_1^2)}{2al_1}\right] \tag{9}$$

To determine the angular velocity ω_1 and angular acceleration ε_1 of the crankshaft, we calculate them by differentiating equation 9 separately:

$$\omega_1 = \frac{d\varphi_1}{dt} = \frac{2B}{\sqrt{4a^2l_1^2-(B^2-(a^2+l_1^2))^2}}\frac{dB}{dt} \tag{10}$$

$$\varepsilon_1 = \frac{d^2\varphi_1}{dt^2} = \frac{2\sqrt{4a^2l_1^2-(B^2-(a^2+l_1^2))^2}+\frac{4B\,(B^2-(a^2+l_1^2))^2}{\sqrt{4a^2l_1^2-(B^2-(a^2+l_1^2))^2}}}{4a^2l_1^2-(B^2-(a^2+l_1^2))^2}\frac{d^2B}{dt^2} = \frac{2(4a^2l_1^2-(B^2-(a^2+l_1^2))^2+4B\,(B^2-(a^2+l_1^2))^2}{\left[4a^2l_1^2-(B^2-(a^2+l_1^2))^2\right]^{3/2}}\frac{d^2B}{dt^2} \tag{11}$$

It is necessary to project the velocity and acceleration of point "A" of the cam mechanism onto the coordinate axes.

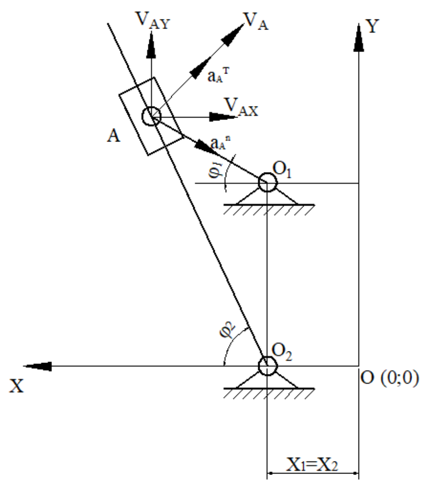

Fig. 3.

We determine the projections of the velocities and accelerations shown in Figure 3 onto the coordinate axis as follows:

$$V_A = \omega_1 l_1 = \frac{2Bl_1}{\sqrt{4a^2l_1^2-(B^2-(a^2+l_1^2))^2}}\frac{dB}{dt} \tag{12}$$

By projecting the function value in equation 12 onto the abscissa and ordinate axes, we obtain the following equalities:

$$V_{AX} = -V_A sin\varphi_1 = \frac{2Bl_1 sin\varphi_1}{\sqrt{4a^2l_1^2-(B^2-(a^2+l_1^2))^2}}\frac{dB}{dt} \tag{13}$$

$$V_{AY} = V_A cos\varphi_1 = \frac{2Bl_1 cos\varphi_1}{\sqrt{4a^2l_1^2-(B^2-(a^2+l_1^2))^2}}\frac{dB}{dt} \tag{14}$$

By projecting the acceleration of point "A" of the crank-slider mechanism, we determine the following:

$$\overrightarrow{a_A} = \overrightarrow{a_A^n} + a_A^\tau;$$

$$a_A = \sqrt{a_A^n + a_A^\tau} \tag{15}$$

$$\overrightarrow{a_X} = \overrightarrow{a_{AX}^n} + a_{AX}^\tau$$
$$\overrightarrow{a_Y} = \overrightarrow{a_{AY}^n} + a_{AY}^\tau \tag{16}$$

The value of the normal acceleration a_A^n, given in formula 15, is determined using the following equation:

$$a_A^n = \omega_1^2 l_1 = \frac{4B^2 l_1}{4a^2 l_1^2 - (B^2 - (a^2 + l_1^2))^2} \left(\frac{dB}{dt}\right)^2 \tag{17}$$

$$a_{AX}^n = -a_A^n \cos\varphi_1 = -\frac{4B^2 l_1 \cos\varphi_1}{4a^2 l_1^2 - (B^2 - (a^2 + l_1^2))^2} \left(\frac{dB}{dt}\right)^2 \tag{18}$$

$$a_{AY}^n = a_A^n \sin\varphi_1 = -\frac{4B^2 l_1 \sin\varphi_1}{4a^2 l_1^2 - (B^2 - (a^2 + l_1^2))^2} \left(\frac{dB}{dt}\right)^2 \tag{19}$$

The tangential acceleration of point A can be determined as follows:

$$a_A^\tau = \varepsilon_1 l_1 = \frac{2l_1(4a^2 l_1^2 - (B^2 - (a^2 + l_1^2))^2 + 4B\,(B^2 - (a^2 + l_1^2))^2}{\left[4a^2 l_1^2 - (B^2 - (a^2 + l_1^2))^2\right]^{3/2}} \frac{d^2B}{dt^2} \tag{20}$$

$$a_{AX}^\tau = -a_A^\tau \sin\varphi_1 = -\frac{2l_1\left(4a^2 l_1^2 - (B^2 - (a^2 + l_1^2))^2\right) + 4B\,(B^2 - (a^2 + l_1^2))^2 \sin\varphi_1}{\left[4a^2 l_1^2 - (B^2 - (a^2 + l_1^2))^2\right]^{3/2}} \frac{d^2B}{dt^2} \tag{21}$$

$$a_{AY}^\tau = a_A^\tau \cos\varphi_1 = -\frac{2l_1\left(4a^2 l_1^2 - (B^2 - (a^2 + l_1^2))^2\right) + 4B\,(B^2 - (a^2 + l_1^2))^2 \cos\varphi_1}{\left[4a^2 l_1^2 - (B^2 - (a^2 + l_1^2))^2\right]^{3/2}} \frac{d^2B}{dt^2} \tag{22}$$

From the resulting system of equations (10) and (11), investigations are conducted using the Mathcad-20 program to analyze the changes in ω_1 and ε_1 per unit time, based on the value of the distance "a" between supports O_1 and O_2 and the length of the crankshaft.

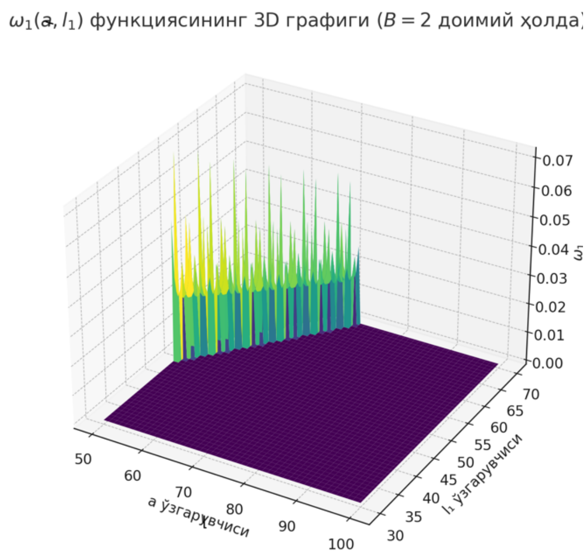

$y_1 = a$ The value ranges from 50 mm to 100 mm,

The value of A=l_1 is in the range from 30 mm to 70 mm, and B remains constant.

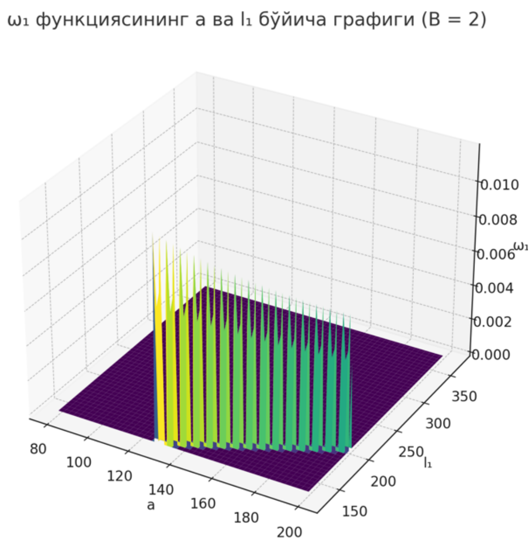

$y_1 = a$ the value ranges from 80 mm to 200 mm,

the value of $O_1A=l_1$ is in the range from 150 mm to 350 mm, and when B remains constant

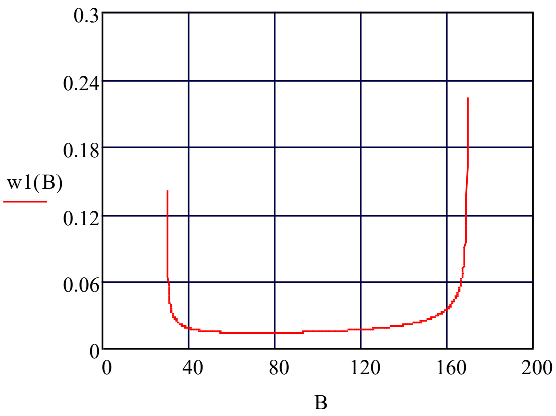

$y_1 = a = 100mm;\ O_1A = l_1 = 70mm$

and when the value of B changes within the range of 0 to 200

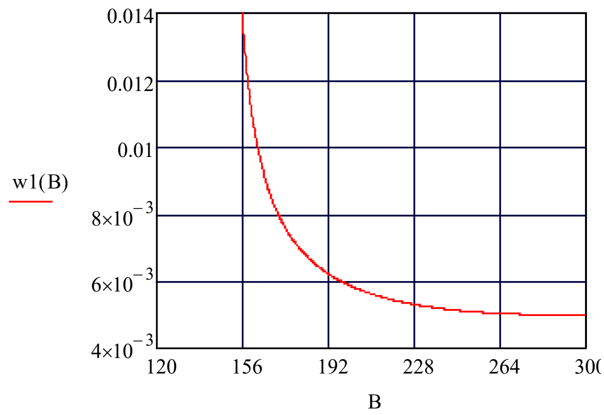

$y_1 = a = 200mm;\ O_1A = l_1 = 350mm$

and when the value of B changes within the range of 0 to 200

Fig. 4. Graph showing the relationship between the angular velocity of the crank mechanism link and the distance between links and supports

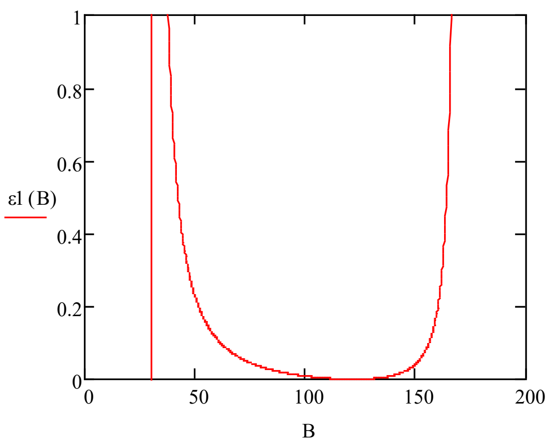

$y_1 = a = 100mm;\ O_1A = l_1 = 70mm$

and when the change value of B is between 0 and 200

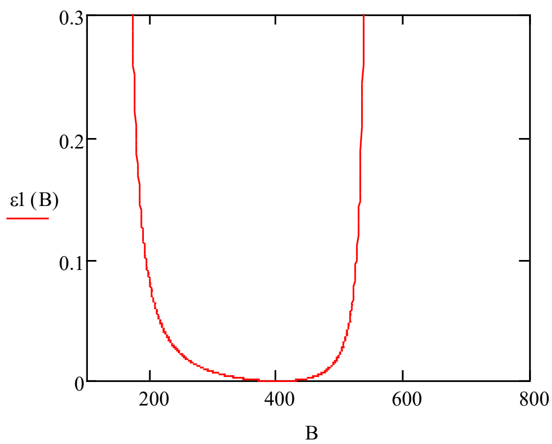

$y_1 = a = 200mm;\ O_1A = l_1 = 350mm$

and when the change value of B is in the range from 200 to 800

Fig. 5. Graph showing the relationship between the angular acceleration of the mechanism's crank link and the distance between links and supports

Using the system of equations 5 and 6, let's examine the change in the rotation angle φ_2 of the coulisse:

$$cos\varphi_1 = b_2 cos\varphi_2 \tag{23}$$

$$sin\varphi_1 = -c_3 + b_2 sin\varphi_2 \tag{24}$$

here, $b_2 = \frac{B}{l_1}$; $c_3 = \frac{a}{l_1}$.

By squaring the left and right sides of equations 23 and 24 and then adding them together, we obtain the following equality:

$$sin\varphi_2 = \frac{b_2^2 + c_3^2 - 1}{2c_3 b_2} \tag{25}$$

Then the value of φ_2 will be equal to:

$$\varphi_2 = \arcsin\left[\frac{b_2^2+c_3^2-1}{2c_3b_2}\right] \tag{26}$$

By substituting the values of the coefficients b_2 and c_3 in equation 26, we obtain the equation for calculating the total angle of rotation φ_2 of the coulisse:

$$\varphi_2 = arcsin\left[\frac{B^2+a^2-l_1^2}{2Ba}\right] \tag{27}$$

To determine the values of angular velocity ω_2 and angular acceleration ε_2 of the crank-slider mechanism, we will use the laws of change for the functions учун $X_1 = X_1(t)$; $X_2 = X_2(t)$; $Y_1 = Y_1(t)$; $Y_2 = Y_2(t)$; and $B = B(t)$

$$\left.\begin{aligned}\omega_2 &= \frac{d\varphi_2}{dt}\\ \varepsilon_2 &= \frac{d^2\varphi_2}{dt^2}\end{aligned}\right\} \tag{28}$$

By first and second-order differentiation of equation 27, we obtain the following equations:

$$\omega_2 = \frac{d\varphi_2}{dt} = \frac{\frac{B}{a}}{\sqrt{\frac{4B^2a^2-(B^2+a^2-l_1^2)^2}{4B^2a^2}}}\frac{dB}{dt} = \frac{2B^2a^2}{\sqrt{4B^2a^2-(B^2+a^2-l_1^2)^2}}\frac{dB}{dt} \tag{29}$$

$$\varepsilon_2 = \frac{d^2\varphi_2}{dt^2} = \frac{4Ba\sqrt{4B^2a^2-(B^2+a^2-l_1^2)^2}-\frac{8Ba^2-2(B^2+a^2-l_1^2)\cdot 2B}{\sqrt{4B^2a^2-(B^2+a^2-l_1^2)^2}}}{4B^2a^2-(B^2+a^2-l_1^2)^2}\frac{d^2B}{dt^2} = \frac{4Ba\left(4B^2a^2-(B^2+a^2-l_1^2)^2\right)-2a^2-(B^2+a^2-l_1^2)}{4B^2a^2-(B^2+a^2-l_1^2)^{3/2}}\frac{d^2B}{dt^2} \tag{30}$$

By calculating the system of equations 29 and 30 above using the MathCad-20 program, we determine the following:

The value of y_1=a ranges from 50 mm to 100 mm,

The value of $O_1A=l_1$ is within the range of 30 mm to 70 mm, while B remains constant.

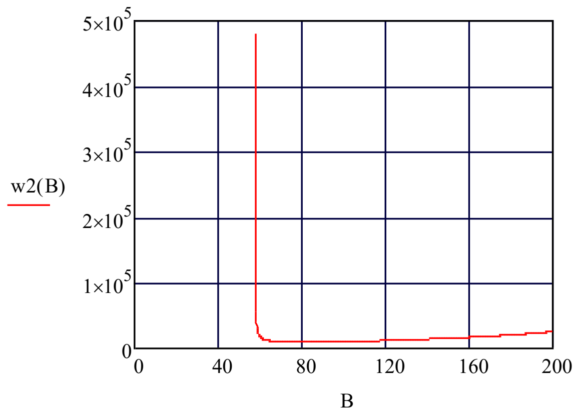

$y_1 = a = 100mm;\ O_1A = l_1 = 70mm$

and when the value of B changes within the range from 0 to 200

The value of y_1=a ranges from 80 mm to 200 mm,

the value of $O_1A=l_1$ is within the range of 150 mm to 350 mm, while B remains constant.

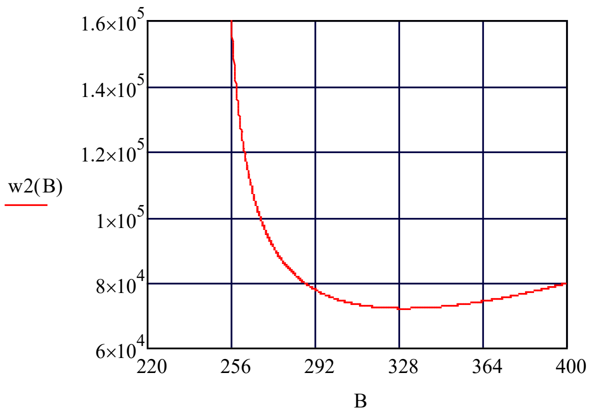

$y_1 = a = 200mm;\ O_1A = l_1 = 350mm$

and when the value of B changes within the range of 220 to 400

Figure 6. Graph depicting the relationship between the angular velocity of the mechanism's rocker arm and the distance between links and supports

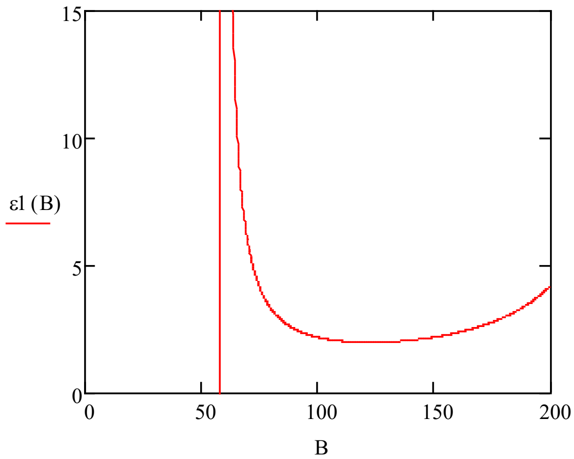

$y_1 = a = 100mm; O_1A = l_1 = 70mm$

and when the change value of B is between 0 and 200

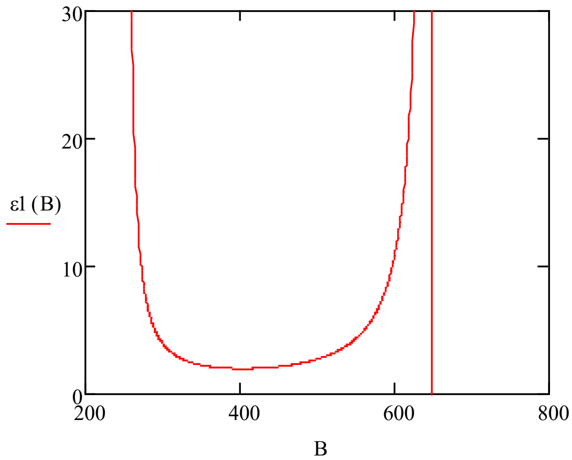

$y_1 = a = 200mm; O_1A = l_1 = 350mm$

and when the change value of B is in the range from 200 to 800

Figure 7. Graph showing the relationship between the angular acceleration of the mechanism's coulisse link and the distance between links and supports

CONCLUSION

When designing a mechanical activator for use in the process of mechanical activation of dispersed fillers in polymer composite materials, it is necessary to optimize its geometric parameters. Therefore, the research conducted on the aforementioned first and second-order differential equations demonstrates that it is possible to determine the optimal values for the distances between the supports of the mechanical activator, as well as the lengths of the crankshaft and slide. In this regard, based on the requirements for mechanical activators, it is possible to determine the optimal indicators of their geometric parameters. For future research work, it will be necessary to determine what speed, acceleration, and centrifugal force should be applied during the mechanical activation of dispersed fillers in polymer composite materials to achieve the desired activation effect.

REFERENCES

1. Duffy, J., Agostini, S., Brown, R., Majewski, C., Marsh, S., & Rudolph, N. (2025). Investigating the effect of glass filler on the aging behavior of polymer powders for additive manufacturing. *International Journal of Polymer Analysis and Characterization*, 1-13.
2. Mamayev, S., Ibadullayev, A., Teshabayeva, E., Tursunaliev, M., & Ikromov, M. A. (2023). Creation of elastomer-based compositions with special characteristics for the wheel-engine block of thermal locomotives. In E3S Web of Conferences (Vol. 452, p. 04013). EDP Sciences.
3. Tambe, P., Tanniru, M., & Sai, B. K. (2022). Structural/load bearing characteristics of polymer-graphene composites. In *Polymer Nanocomposites Containing Graphene* (pp. 379-400). Woodhead Publishing.
4. Ziyamukhamedova, U., Djumabaev, A., Urinov, B., & Almatayev, T. (2021). Features of structural adaptability of polymer composite coatings. In *E3S Web of Conferences* (Vol. 264, p. 05011). EDP Sciences.

5. Ziyamukhamedova, U., Djumabaev, D., & Shaymardanov, B. (2013). Mechanochemical modification method used in the development of new composite materials based on epoxy binder and natural minerals. *Turkish journal of Chemistry*, *37*(1), 51-56.

6. Bakhtiari, S. S. E., Shyha, I., Sun, D., Nofar, M., & Salehiyan, R. (2025). Re-evaluating bioplastic blend wastes through mechanical recycling and chemical modification. *Advanced Industrial and Engineering Polymer Research*.

7. Lin, Z., Sun, Z., Fu, W., Lin, Y. C., Moon, K. S., & Wong, C. P. (2025). Thermally conductive and electrically insulative alumina/epoxy composites for advanced electronic packaging applications: A comprehensive review of filler morphologies and surface modifications. *Materials Today*.

8. Ziyamukhamedova, U., Evlen, H., Nafasov, J., Jalolova, Z., Turgunaliyev, E., & Rakhmatov, E. (2023). Modeling of the process of mechano activation of filler particles in polymer composites. In *E3S Web of Conferences* (Vol. 401, p. 05027). EDP Sciences

9. Mamaev, S., Anna, A., Tursunov, S., Nigmatova, D., & Tursunov, T. (2023). Mathematical modeling of torsional vibrations of the wheel-motor unit of mains diesel locomotive UZTE16M. In *E3S Web of Conferences* (Vol. 401, p. 05014). EDP Sciences.

10. Mamayev, S., Avdeeva, A., Ablyalimov, O., & Nigmatova, D. (2023). Optimization of the operation of the mechanism of the cross planer. In E3S Web of Conferences (Vol. 401, p. 05026). EDP Sciences.

11. Mamayev, S., Ibadullayev, A., Nigmatova, D., Teshabayeva, E., & Tursunaliev, M. (2023). Creation of special compositions based on butadiene-nitrile elastomers for diesels. In E3S Web of Conferences (Vol. 401, p. 03028). EDP Sciences.